
Article:
Luo, P. and Madathil, S.N.E. orcid.org/0000-0001-6832-1300 (2020) Theoretical analysis of on-state performance limit of 4H-SiC IGBT in field-stop technology. IEEE Transactions on Electron Devices, 67 (12). pp. 5621-5627. ISSN 0018-9383

https://doi.org/10.1109/TED.2020.3033268

Theoretical Analysis of On-state Performance Limit of 4H-SiC IGBT in Field-Stop Technology

Peng Luo, *Member, IEEE*, and E. M. S. Narayanan, *Senior Member, IEEE*

***Abstract*—In this paper, the on-state performance limits of 4H-SiC IGBTs are theoretically estimated for the first time and compared against silicon counterparts. The theoretical analysis is based on the static modelling of a high-current PiN diode and the calculation results are examined with TCAD simulations. Owing to conductivity modulation effect, the on-state losses of 4H-SiC IGBTs do not show any significant increase with the increase in breakdown voltage. However, the large built-in potential of SiC poses an inherent limit on the reduction of on-state voltage drop. Compared with 4H-SiC IGBTs, the silicon based IGBTs exhibit superior on-state performance limits within the breakdown voltage range considered, although their drift layer thicknesses are 10 times higher than that of 4H-SiC IGBTs. Therefore, silicon IGBTs remain as efficient technologies for enhancing high power conversion efficiency.**

***Index Terms*—IGBT, silicon carbide, 4H-SiC IGBT, theoretical limit, forward voltage drop, injection efficiency.**

I. Introduction

SILICON Carbide (SiC) based power devices are well suited for high voltage power electronics by taking the advantages of its superior physical and electrical properties, such as high critical electric field, high electron velocity and high thermal conductivity. Owing to the remarkable progress in material growth and device technologies, SiC unipolar devices have been introduced commercially from 600 V to 1700 V [1-3]. The first commercial SiC power device was a Schottky Barrier Diode (SBD), which was released in 2001 [4]. After the improvement of channel mobility and gate oxide reliability, a 1.2 kV planar type SiC MOSFET became commercially available in 2011 [3] and the trench type SiC MOSFET was reported in 2015 [5]. The highest blocking voltage reported so far is the 15 kV SiC MOSFETs [6], which have been used in developing high frequency solid-state transformers [7]. Although the SiC MOSFETs have exhibited superior high frequency switching performance in comparison to Si-IGBTs, the on-state losses increase dramatically when blocking voltage is higher than 10 kV. Moreover, the specific on-resistance ($R_{on,sp}$) further increases with increasing junction temperature due to reduced carrier mobility. Therefore, using ultra-high voltage (> 10 kV) unipolar devices for high power applications is not a cost-effective solution from the practical point of view.

To operate beyond the 1-D material limit for SiC unipolar devices, SiC bipolar devices such as 4H-SiC IGBTs with blocking voltages from 5.8 kV to 27 kV have been developed to achieve a much higher current density [8-30]. The first 4H-SiC IGBT was reported in 1999 [8] and the early fabricated SiC IGBTs were mostly p-channel type due to easy availability and low resistance of n^+ substrates [30]. After SiC epitaxial growth and fabrication technologies became mature, n-channel SiC IGBTs were developed with thick free-standing SiC epitaxial layers and various substrate removal/grinding processes [19, 24, 27, 29]. As the electron mobility is nearly 8 times higher than the hole mobility in 4H-SiC, n-channel IGBTs are more favored than p-channel IGBTs due to lower on-state voltage drops and faster switching speeds [21, 31]. However, the large built-in potential induced by the wide bandgap of SiC (3.26 eV) is still a primary limitation to the on-state performance. Another challenge is the low ambipolar lifetime which is generally on the order of 1 μs [28]. Without high ambipolar lifetime, the diffusion lengths of the carriers are not sufficient to generate high levels of conductivity modulation within the drift regions. Recent efforts on lifetime enhancement procedures have confirmed that long time (10 ~15 hours) thermal oxidation at 1300 ºC can improve the as-grown drift ambipolar lifetime to more than 10 μs [28, 32, 33]. Such high carrier lifetime can result in a higher level of conductivity modulation in the SiC bipolar devices and enable the blocking voltages of 4H-SiC IGBTs to be further increased. In the meantime, the developments on silicon-based power devices have shown significant progress in terms of power efficiency as well as blocking capability. For example, a silicon IGBT device in planar gate and Soft-Punch-Through (SPT) technologies has shown a breakdown voltage of 8.4 kV with superior on-state performance and short-circuit capability [34]. In addition, the silicon Light-Triggered Thyristors (LTT) with conventional field-stop layers can yield a blocking capability of more than 13 kV [35, 36]. Recently, the feasibility study of a 13 kV silicon IGBT was discussed [37]. The proposed device can be operated under a DC voltage of 6.6 kV and at a switching frequency of 150 Hz. Therefore, it becomes imperative to investigate the on-state performance limit of 4H-SiC IGBTs with comparison to the theoretical limit of silicon-based IGBTs (Si-IGBTs) [38].

Manuscript received ; revised ; accepted . Date of current version . Recommended for publication by Associate Editor

The authors are with the Electrical Machines and Drives Research Group, Department of Electronic and Electrical Engineering, University of Sheffield, S1 3JD, U.K. (email: pluo2@sheffield.ac.uk; s.madathil@sheffield.ac.uk).

Color versions of one or more of the figures in this paper are available on line at http://ieeexplore.ieee.org.

Digital Object Identifier

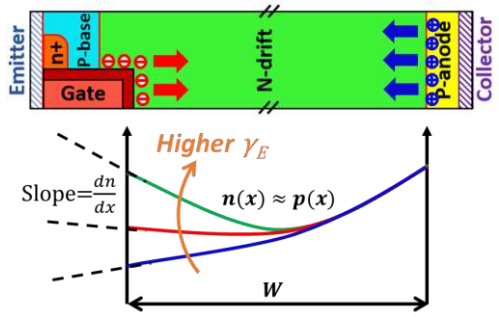

Fig. 1. Charge distributions within an IGBT.

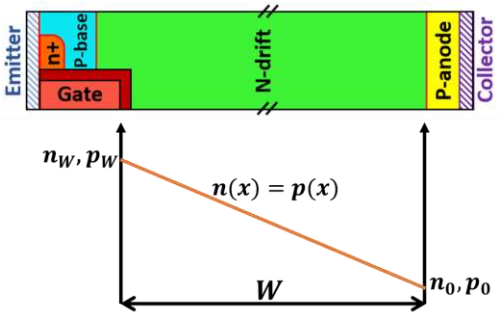

Fig. 2. Ideal on-state carrier distribution within an IGBT.

In this paper, the ideal on-state performance of an IGBT is analyzed through static modeling of a high current PiN diode in Section III. Section IV compares the on-state performance limits between 4H-SiC IGBTs and Si-IGBTs. In Section V, TCAD simulations are employed to examine the proposed theoretical limits. Finally, the theoretical analysis and the simulation work are summarized in Section VI.

II. Ideal Performance of an IGBT

Fig. 1 shows the on-state charge distributions within an IGBT. The theory of achieving the lowest forward voltage drops in a PiN diode or an IGBT has been proposed in [38, 39]. As per this model, electrons are injected from channel inversion layers and accumulated beneath the trench gate, a PiN diode structure is thus formed within the IGBT. Since the channel resistance of an IGBT is largely dependent on the MOS structure design and the channel mobility, the improvement of the on-state behavior of an IGBT is mainly focused on improving the carrier distribution within the N-drift layer. For a definite current density, a higher carrier density within the drift region is desirable to obtain a lower forward voltage drop ($V_{ce(sat)}$). The electron injection efficiency (γ_E) is defined as the ratio of the electron current density to the total current density, as shown in (1). Assuming bipolar condition ($n \approx p$) is satisfied within the drift layer and eliminating the parameter of electric field (E) from (2)-(4), the slope of the excess carrier profiles at the cathode side can be expressed as (5). Therefore, it can be concluded that the IGBT structure performs the lowest $V_{ce(sat)}$ when the γ_E is close to 1.

$$\gamma_E = \frac{J_n}{J} = \frac{J_n}{J_p + J_n} \tag{1}$$

$$J_p = qp\mu_p E - qD_p \frac{dp}{dx} \tag{2}$$

$$J_n = qn\mu_n E + qD_n \frac{dn}{dx} \tag{3}$$

$$D_{n,p} = \left(\frac{kT}{q}\right)\mu_{n,p} \tag{4}$$

$$\frac{dn}{dx} = \frac{J(\mu_n + \mu_p)}{2kT\mu_n\mu_p} \cdot \left(\gamma_E - \frac{\mu_n}{\mu_n + \mu_p}\right) \tag{5}$$

III. Static Modelling of an IGBT

The $V_{ce(sat)}$ of a trench IGBT structure consists of three components: 1) junction voltage (V_J), 2) drift voltage (V_{drift}) and 3) the voltage drop (V_{ch}) across the channel resistance (R_{ch}). As per the analysis in Section II, the ideal on-state performance can be assumed that all of the current is conducted by electrons (γ_E = 1). In addition, it was found that the forward voltage drop can be significantly reduced by making the charge profile of the drift region feature a decrease from cathode side to anode side [39]. Therefore, the anode injection efficiency is low and the excess carrier profile within the i-layer/drift-layer is assumed to exhibit a linear decrease from cathode side to anode side, as depicted in Fig. 2. It is also assumed herein that the carrier lifetimes are long enough and there is no recombination within the N-drift region [38, 39]. As the hole current is absent ($J_p = 0$), the electric field can be expressed as (6). Thus, the V_{drift} can be obtained by integrating the electric field within the N-drift region, as shown in (7). In addition, the V_J consists of the voltage across the P-anode/N-drift junction (J_1) and the voltage across the accumulation layer/N-drift interface (J_2), as expressed in (8)-(10), where the p_0' and n_W' are the hole and electron concentration at J_1 and J_2 under equilibrium, respectively. Therefore, the minimum $V_{ce(sat)}$ can be derived with the distributed carrier concentration (n_0 and n_W), which can be calculated by integrating (11). According to the assumption in [39], the n_0 can be expressed as (12), where Q_{pa} and D_{n0} are the P-anode dose and electron diffusion coefficient in the P-anode, respectively. $D_n(n)$ can be described with the carrier-carrier scattering mobility proposed for a germanium diode [40, 41], as shown in (13)-(15), where m_n and m_p are the density-of-state effective masses for electron and hole, respectively. As described in [39], the $D_n(n)$ can be further simplified as (16)-(18), where n_m is the maximum electron concentration within the N-drift region. At last, the carrier distribution ($n(x)$) shown in (19) is calculated with (11), (12) and (16). The minimum $V_{ce(sat)}$ of an IGBT device considered V_{ch} is finally expressed in (20).

$$E = \frac{kT}{q}\frac{1}{n}\frac{dn}{dx} \tag{6}$$

$$V_{drift} = \int_0^W E\,dx = \frac{kT}{q}\ln\frac{n_W}{n_0} \tag{7}$$

$$V_{J1} = \frac{kT}{q}\ln\frac{p_o}{p_0'} \tag{8}$$

$$V_{J2} = \frac{kT}{q}\ln\frac{n_W}{n_W'} \tag{9}$$

$$V_J = V_{J1} + V_{J2} = \frac{kT}{q}\ln\frac{n_o n_W}{n_i^2} \tag{10}$$

$$D_n(n)\frac{dn}{dx} = \frac{J_n}{2q} = \frac{J}{2q} \tag{11}$$

$$n_0 = \sqrt{Q_{pa}J/qD_{n0}} \tag{12}$$

$$\mu_n = \frac{q}{kT}D_n = \frac{q}{kT}\frac{B}{n\ln(A/n)} \tag{13}$$

$$A = \frac{2.07\times10^{15}\times T^2}{m_n^{-1}+m_p^{-1}} \tag{14}$$

$$B = 2.16\times10^{13}\times(m_n^{-1}+m_p^{-1})^{1/2}\times T^{5/2} \tag{15}$$

$$D_n(n) = a/(n+b) \tag{16}$$

$$a = B/\left\{\left(1+\ln\frac{A}{n_m}\right)+\left(1+\ln\frac{A}{n_m}\right)^{-1}\right\} \tag{17}$$

$$b = a/D_n(0) = a/D_{n0} \tag{18}$$

$$n(x) = \left(\sqrt{\frac{Q_{pa}J}{qD_{n0}}}+b\right)e^{\left(\frac{Jx}{2qa}\right)}-b \tag{19}$$

$$V_{ce(sat)} = V_{drift}+V_J+V_{ch} = \frac{2kT}{q}\ln\frac{n_W}{n_i}+R_{ch}J$$
$$= \frac{2kT}{q}\ln\left[\frac{1}{n_i}\left\{\left(\sqrt{\frac{Q_{pa}J}{qD_{n0}}}+b\right)e^{\left(\frac{Jx}{2qa}\right)}-b\right\}\right]+R_{ch}J \tag{20}$$

TABLE I
ELECTRICAL PROPERTIES OF SILICON AND 4H-SIC

Properties ***(T_j = 25 ºC / 125 ºC)***	***Silicon***	***4H-SiC***
Energy Bandgap (eV)	1.12 / 1.09 [42]	3.26 / 3.23 [4]
Intrinsic carrier concentration n_i (cm^{-3})	1×10^{10} / 6.16×10^{12} [42]	1.73×10^{-8} / 0.24 [4]
Electron mobility μ_n (cm^2/Vs)	1450 / 715 [43]	950 / 476 [44]
Electron diffusion coefficient D_{n0} (cm^2/s)	37.4 / 24.6	24.5 / 16.37
Electron density-of-state effective mass m_n (m_0^{-1})	1.18 / 1.22 [42]	0.4 / 0.41 [45]
Hole density-of-state effective mass m_p (m_0^{-1})	0.81 / 0.85 [42]	2.64 / 2.65 [45]
Maximum electron concentration n_m (cm^{-3})	1×10^{18}	1×10^{17}
P-anode dose Q_{pa} (cm^{-2})	5×10^{13}	3×10^{15}

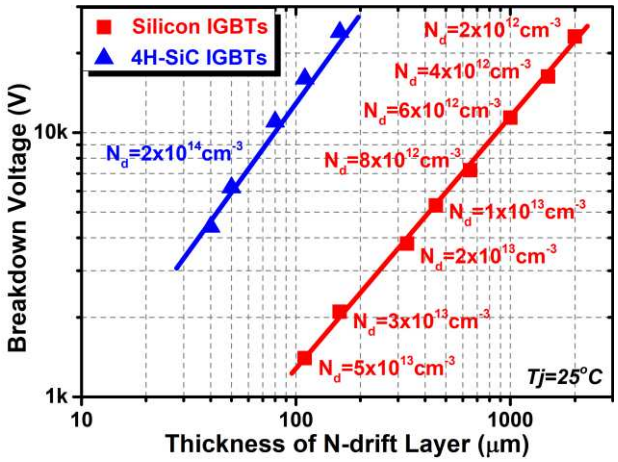

Fig. 3. Dependence of breakdown voltage on the N-drift thickness and doping concentration at T_j = 25 ºC.

IV. Performance Limits of 4H-SIC IGBTs

To calculate the on-state performance limits of Si-IGBTs and 4H-SiC IGBTs, the electrical properties of silicon and 4H-SiC are listed in Table I. The N-drift thickness (W) used for calculation is considered as the drift layer thickness of field-stop IGBTs. Fig. 3 shows the dependence of breakdown voltage on W and N-drift doping concentration (N_d). As the critical electric field strength of the 4H-SiC is almost 10 times higher than that of silicon, the 4H-SiC IGBT can achieve an equivalent breakdown voltage with only 1/10 of the drift thickness of a Si-IGBT. In addition, it should be noted that the N_d required for Ultra-High Voltage (UHV) Si-IGBTs (> 10 kV) is lower than the silicon intrinsic carrier concentration (n_i) at T_j = 125 ºC, as shown in Table I. Therefore, the n_i poses a fundamental limit on the maximum operating temperature of UHV Si-IGBTs. In contrast, 4H-SiC IGBTs do not suffer from this issue owing to the much lower n_i as a result of wider energy bandgap. Hence, a much higher operating temperature can be achieved by 4H-SiC IGBTs from the blocking capability point of view. On the other hand, the Auger recombination and band-to-band (radiative) recombination have a significant impact on the effective carrier lifetime at high injection levels [46]. Therefore, the maximum excess carrier density (n_m) must take Auger recombination and band-to-band recombination into account. In the theoretical investigation of Si-IGBT performance limit [38], the excess carrier density is in the range of 1×10^{17} to 1×10^{18} cm^{-3} at high current densities, and the diffusion coefficient is significantly reduced compared with the simulation results when the carrier density is higher than 1×10^{18} cm^{-3}. Thus, the maximum electron density considered herein is 1×10^{18} cm^{-3} for the analysis of Si-IGBT performance limits. However, in the ultra-high voltage 4H-SiC PiN diodes, the band-to-band recombination significantly reduces the effective carrier lifetime when the excess carrier concentration is higher than 1×10^{17} cm^{-3} [46], which poses an inherent limit on the on-state performance. As shown in Fig. 6(b) and Fig. 7, the excess carrier density within a 110 μm drift layer is in the range

TABLE II
CHANNEL PARAMETERS

Parameters (T_j = 25 ºC / 125 ºC)	*Si-IGBTs*	*4H-SiC IGBTs*
Channel mobility μ_{ch} (cm²/V·s)	300 / 200 [47]	18 / 20 [17]
Cell pitch W_{cell} (µm)	14.5	14.5 [17]
Channel length L_{ch} (µm)	0.7	0.7 [17]
Gate oxide thickness t_{ox} (nm)	50	50 [17]
Gate voltage V_g (V)	20	20 [17]
Threshold voltage V_{th} (V)	3 / 2	3 / 2 [17]
Channel resistance R_{ch} (mΩ*cm²)	0.14 / 0.2	2.37 / 2.01

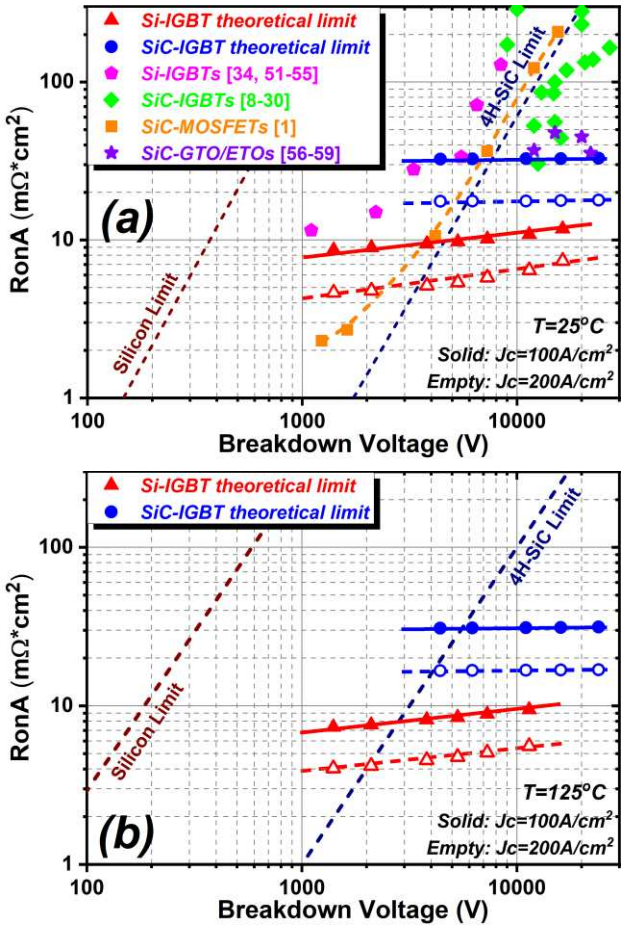

Fig. 4. Theoretical limits of Si-IGBT and 4H-SiC IGBT at (a) T_j = 25 ºC and (b) T_j = 125 ºC.

$$R_{ch} = \frac{W_{cell} L_{ch}}{2\mu_{ch} C_{ox} (V_g - V_{th})} \tag{21}$$

of 1×10^{16} to 1×10^{17} cm^{-3} at J_c = 100 A/cm^2, the estimated ambipolar diffusion length in this case is about 100 µm [46], which is sufficient to highly modulate the conductivity of a drift layer below 200 µm [48]. Therefore, the maximum electron density used for 4H-SiC IGBTs is 1×10^{17} cm^{-3}.

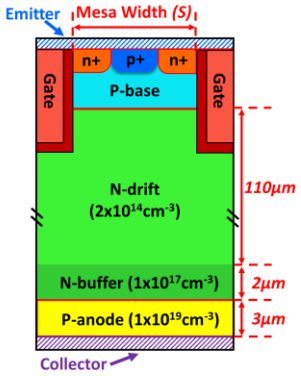

Fig. 5. Cross-section of a simulated 15-kV trench field-stop 4H-SiC IGBT.

Moreover, the low channel mobility of 4H-SiC IGBTs results in a high channel resistance [14, 15, 17], which cannot be ignored in the analysis of on-state performance. The channel resistance can be calculated with (21), assuming that channel parameters are constant across the voltage range considered, and the channel layers are not conductivity modulated even in the narrow mesa IGBTs [49, 50]. Table II summarizes the channel parameters for Si-IGBTs and 4H-SiC IGBTs. The channel parameters for 4H-SiC IGBTs are from the experimental data in [17], and the main parameters are kept constant for comparison. Due to the lower channel mobility, the R_{ch} of 4H-SiC IGBTs is 10 times higher than that of Si-IGBTs.

Figs. 4 (a) and (b) compare the on-state performance limits between Si-IGBTs and 4H-SiC IGBTs at T_j = 25 ºC and T_j = 125 ºC, respectively. The absolute specific on-resistances ($R_{on,sp}$) are calculated at J_c = 100 A/cm^2 and J_c = 200 A/cm^2, respectively. In addition, the experimental data of the Si-IGBTs [34, 51-55], SiC IGBTs [8-30], SiC MOSFETs [1] and SiC GTOs/ETOs [56-59] are plotted in Fig. 4(a). In comparison to the unipolar devices, the $R_{on,sp}$ of Si-IGBTs and 4H-SiC IGBTs are not sensitive to the variation in breakdown voltage owing to the conductivity modulated drift layers. Although both 4H-SiC IGBT experimental data and performance limits have shown significant improvement of $R_{on,sp}$ compared to that of SiC MOSFETs for UHV (> 10 kV) cases, the theoretical limits of 4H-SiC IGBTs are still much higher than that of Si-IGBTs when BV < 20 kV due to the large built-in potential (knee voltage). This is the case even at T_j = 125 ºC although the built-in potential has decreased at high temperature. However, the UHV Si-IGBTs (> 10 kV) are lack of high temperature operation (T_j > 125 ºC) capability due to the inherent limit on breakdown voltage. In contrast, owing to the much lower intrinsic carrier densities at high temperatures, 4H-SiC IGBTs can remain high temperature operation capability without any impact on the blocking stability. Note that some experimental data of SiC IGBTs shown in Fig. 4(a) are close to the SiC-IGBT limit at J_c = 100 A/cm^2, because they are operated at current densities of more than 100 A/cm^2. However, they are still much higher than the theoretical limit at J_c = 200 A/cm^2. Therefore, there is still large room for SiC IGBTs to be further improved. Moreover, recent research showed that the channel mobility of a lateral trench SiC MOSFET can be significantly increased to 276 cm^2/V·s due to FinFET effect [60]. Hence, the on-state

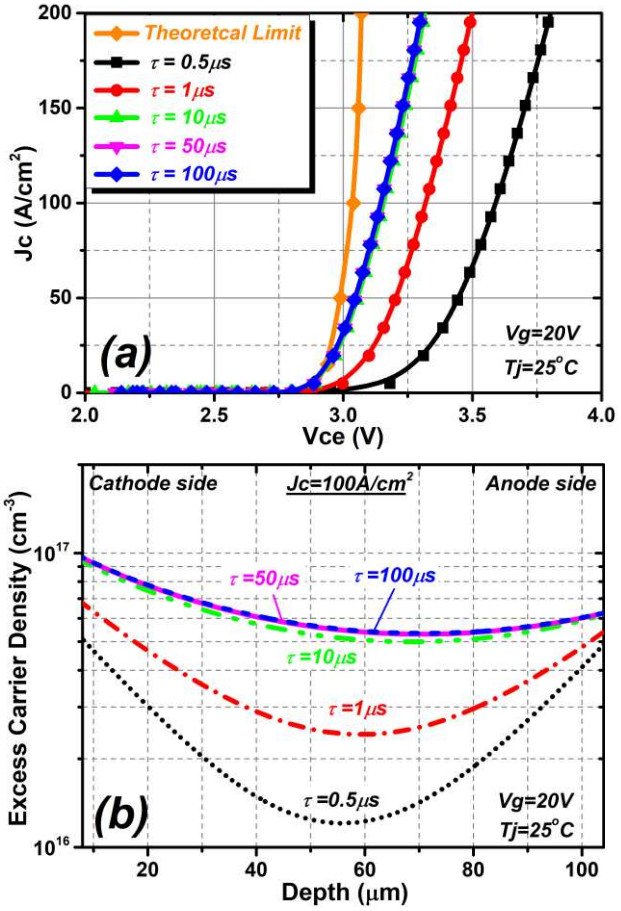

Fig. 6. Influence of carrier lifetime upon (a) I -V characteristics and (b) excess carrier distributions during on-state, mesa width S = 0.1 μm.

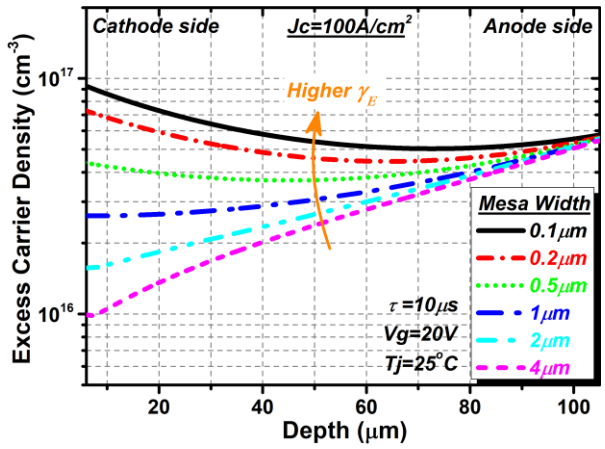

Fig. 7. Influence of γ_E upon the on-state carrier density within the N-drift layer, trench width is kept identical for comparison.

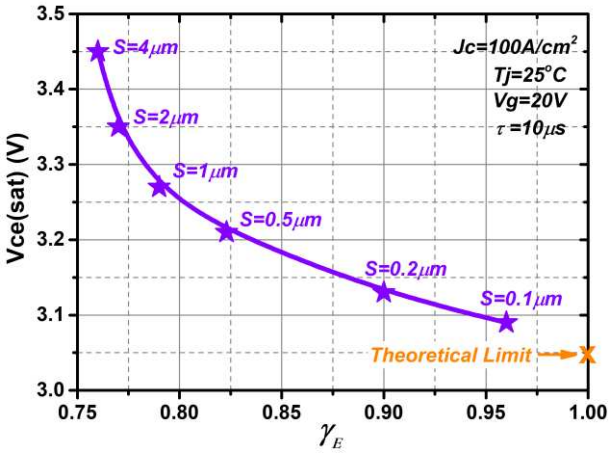

Fig. 8. Influence of γ_E upon the $V_{ce(sat)}$ of the 15 kV 4H-SiC IGBT. The theoretical limit is calculated with a N-drift thickness of 110 μm.

performance of trench SiC IGBTs is expected to be further improved by utilizing the technology in [60].

V. Simulation of 4H-SIC IGBT

A 15 kV 4H-SiC IGBT in field-stop and trench technologies is simulated through Silvaco TCAD [61] to examine the proposed performance limits. The cross-section of the simulated device and the structural parameters are shown in Fig. 5. The thickness of the N-drift region is designed to be 110 μm in order to support more than 16 kV blocking voltage. Physical models including bandgap narrowing model, Shockley-Read-Hall (SRH) recombination and direct recombination (Auger) models [61] are specified within the simulations. Figs. 6 (a) and (b) show the influence of various carrier lifetimes upon I -V characteristics and on-state carrier distributions within the N-drift region, respectively. The carrier lifetime specified in the simulations is the SRH lifetime, which is independent of excess carrier density [46]. As expected, increasing carrier lifetime can effectively improve the I -V performance due to the increase of excess carrier density within the N-drift layer. However, the I -V characteristics do not exhibit any further improvement when the carrier lifetime is increased to more than 10 μs. This is because the direct recombination limits the effective carrier lifetime at high level injection. Fig. 7 shows the influence of γ_E on the on-state carrier density. The cathode side carrier density increases significantly with the increase in γ_E. The increase of γ_E is due to the Injection Enhancement (IE) effect [62], which is achieved by scaling down the mesa width in this case. Smaller mesa width can constrict the flow of hole current into the emitter. Hence, more excessive holes pile up beneath trench corners, which increases the drift layer potential and enhances the electron current from the inversion layers. In addition, the influence of the γ_E upon $V_{ce(sat)}$ is depicted in Fig. 8. It can be seen that the $V_{ce(sat)}$ decreases dramatically with increased γ_E and approaches the theoretical limit when γ_E is close to 1. The calculated $V_{ce(sat)}$ is 3.04 V at J_c = 100 A/cm^2 and T_j = 25 ℃, which is slightly lower than the minimum $V_{ce(sat)}$ (3.09 V) obtained from simulation results. The slight difference is due to the occurrence of direct recombination in the simulations. However, if the direct recombination model is disabled in the simulations, the minimum simulated $V_{ce(sat)}$ will decrease to 3.04 V, which is closely matched with the theoretical calculation. Therefore, it can be concluded that the theoretical analysis regarding to the on-state performance limits of 4H-SiC IGBTs is consistent with the numerical simulation results.

Figs. 9 (a) and (b) compare the theoretical analysis of V_{drift} in this paper with the theoretical analysis of V_{drift} (Equation 7.51)

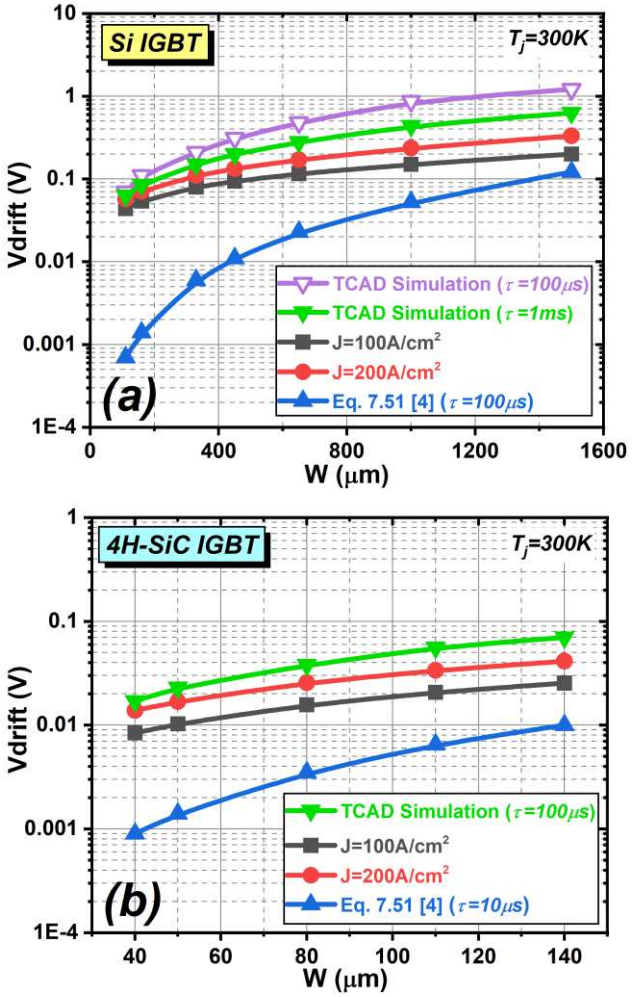

Fig. 9. Comparison of calculated V_{drift} with TCAD simulation results and the theoretical analysis in [4] of (a) Si-IGBT and (b) 4H-SiC IGBT. The simulation results are the V_{drift} of a PiN structure at J_c = 200 A/cm^2.

in the textbook [4]. TCAD simulation results are used as benchmark to examine the proposed on-state limits herein and the theoretical analysis (Equation 7.51) in [4]. Note that the Equation 7.51 in [4] assumes unity injection efficiency at both cathode and anode sides, and the analysis is independent of current density. As shown in Fig. 9, the calculation results in this paper are close to the simulation results and the estimated V_{drift} increases with increasing current density. However, the Eq. 7.51 results are at least one order of magnitude lower than the simulation results, which are over low to estimate the on-state performance limits. This is because unity injection efficiency at anode side is difficult to realize because the field-stop layer limits the P-anode injection efficiency. Therefore, the theoretical analysis herein provides a more accurate method to estimate the on-state performance limits of IGBTs in Field-Stop technology.

VI. Conclusion

The on-state performance limits of 4H-SiC IGBTs in Field-Stop technology are presented and investigated through theoretical analysis and TCAD simulations. Owing to the superior material properties, 4H-SiC IGBTs can provide high temperature operations at UHV conditions and the $R_{on,\,sp}$ does not show any significant increase with the increase in breakdown voltage due to conductivity modulation effect. However, the large built-in potential of 4H-SiC is the major limitation to the on-state performance in the temperature range considered. Simulation results show that the $V_{ce(sat)}$ of 4H-SiC IGBT can be reduced with increased carrier lifetime and tends to be saturated when carrier lifetime is longer than 10 μs. In addition, the on-state behavior can be improved by increasing γ_E. In comparison to the 4H-SiC IGBTs, silicon IGBTs show much lower on-state losses from the performance limit point of view, although their N-drift thicknesses are 10 times higher than that of 4H-SiC IGBTs. Therefore, the silicon-based IGBTs are still competitive in applications below 13 kV, due to the superior on-state behavior and much lower material cost, particularly as many of the UHV applications which do not require fast switching and high temperature operation capabilities.

References

[1] J. W. Palmour, "Silicon carbide power device development for industrial markets," in *IEDM Tech. Dig.*, Dec. 2014, pp. 1.1.1-1.1.8, doi: 10.1109/IEDM.2014.7046960.

[2] T. Kimoto, "Progress and future challenges of silicon carbide devices for integrated circuits," in *Proceedings of the IEEE 2014 Custom Integrated Circuits Conference*, Sep. 2014, pp. 1-8, doi: 10.1109/CICC.2014.6946035.

[3] X. She, A. Q. Huang, L. Ó, and B. Ozpineci, "Review of Silicon Carbide Power Devices and Their Applications," *IEEE Transactions on Industrial Electronics,* vol. 64, no. 10, pp. 8193-8205, Oct. 2017, doi: 10.1109/TIE.2017.2652401.

[4] T. Kimoto and J. A. Cooper, *Fundamentals of silicon carbide technology : growth, characterization, devices and applications*. Singapore: John Wiley & Sons Singapore Pte. Ltd., 2014. doi: 10.1002/9781118313534.

[5] "1200 V/180 A Full SiC PowerModule with Integrated SiC Trench MOSFET" Apr. 2015. Available: www.rohm.com [Online].

[6] V. Pala, E. V. Brunt, L. Cheng, M. O. Loughlin, J. Richmond, A. Burk, S. T. Allen, D. Grider, J. W. Palmour, and C. J. Scozzie, "10 kV and 15 kV silicon carbide power MOSFETs for next-generation energy conversion and transmission systems," in *IEEE Energy Conversion Congress and Exposition (ECCE)*, Sep. 2014, pp. 449-454, doi: 10.1109/ECCE.2014.6953428.

[7] A. Q. Huang, L. Wang, Q. Tian, Q. Zhu, D. Chen, and Y. Wensong, "Medium voltage solid state transformers based on 15 kV SiC MOSFET and JBS diode," in *IECON 2016 - 42nd Annual Conference of the IEEE Industrial Electronics Society*, Oct. 2016, pp. 6996-7002, doi: 10.1109/IECON.2016.7793121.

[8] R. Singh, S. Ryu, and J. W. Palmour, "High temperature, high current, p-channel UMOS 4H-SiC IGBT," in *57th Annual Device Research Conference Digest*, Jun. 1999, pp. 46-47, doi: 10.1109/DRC.1999.806318.

[9] R. Singh, R. Sei-Hyung, D. C. Capell, and J. W. Palmour, "High temperature SiC trench gate p-IGBTs," *IEEE Trans. Electron Devices,* vol. 50, no. 3, pp. 774-784, Jun. 2003 doi: 10.1109/TED.2003.811388.

[10] Q. Zhang, H. Chang, M. Gomez, C. Bui, E. Hanna, J. A. Higgins, T. Isaacs-Smith, and J. R. Williams, "10kV Trench Gate IGBTs on 4H-SiC," in *Proc. 17th Int. Symp. Power Semiconductor Devices and IC's (ISPSD)*, May 2005, pp. 303-306, doi: 10.1109/ISPSD.2005.1488011.

[11] Q. Zhang, C. Jonas, S. Ryu, A. Agarwal, and J. Palmour, "Design and Fabrications of High Voltage IGBTs on 4H-SiC," in *Proc. 18th Int. Symp. Power Semiconductor Devices and IC's (ISPSD)*, Jun. 2006, pp. 1-4, doi: 10.1109/ISPSD.2006.1666127.

[12] Q. Zhang, C. Jonas, R. Callanan, J. Sumakeris, M. Das, A. Agarwal, J. Palmour, S. Ryu, J. Wang, and A. Huang, "New Improvement Results on 7.5 kV 4H-SiC p-IGBTs with $R_{diff,on}$ of 26 mΩ·cm^2 at 25°C," in *Proc.*

19th Int. Symp. Power Semiconductor Devices and IC's (ISPSD), May 2007, pp. 281-284, doi: 10.1109/ISPSD.2007.4294987.

[13] Y. Sui, X. Wang, and J. A. Cooper, "High-Voltage Self-Aligned p-Channel DMOS-IGBTs in 4H-SiC," *IEEE Electron Device Lett.,* vol. 28, no. 8, pp. 728-730, Jul. 2007, doi: 10.1109/LED.2007.901582.

[14] Q. C. J. Zhang, C. Jonas, B. Heath, M. K. Das, S. H. Ryu, A. K. Agarwal, and J. W. Palmour, "9 kV 4H-SiC IGBTs with 88 mΩ·cm^2 of $R_{diff, on}$," *Materials Science Forum,* vol. 556-557, pp. 771-774, Sep. 2007, doi: 10.4028/www.scientific.net/MSF.556-557.771.

[15] Q. Zhang, J. Wang, C. Jonas, R. Callanan, J. J. Sumakeris, S. Ryu, M. Das, A. Agarwal, J. Palmour, and A. Q. Huang, "Design and Characterization of High-Voltage 4H-SiC p-IGBTs," *IEEE Trans. Electron Devices,* vol. 55, no. 8, pp. 1912-1919, Jul. 2008, doi: 10.1109/TED.2008.926627.

[16] Q. Zhang, M. Das, J. Sumakeris, R. Callanan, and A. Agarwal, "12-kV p-Channel IGBTs With Low On-Resistance in 4H-SiC," *IEEE Electron Device Lett.,* vol. 29, no. 9, pp. 1027-1029, Aug. 2008, doi: 10.1109/LED.2008.2001739.

[17] M. K. Das, Q. J. Zhang, R. Callanan, C. Capell, J. Clayton, M. Donofrio, S. K. Haney, F. Husna, C. Jonas, J. Richmond, and J. J. Sumakeris, "A 13 kV 4H-SiC n-Channel IGBT with Low $R_{diff,on}$ and Fast Switching," *Materials Science Forum,* vol. 600-603, pp. 1183-1186, Jan. 2009, doi: 10.4028/www.scientific.net/MSF.600-603.1183.

[18] Q. J. Zhang, C. Jonas, J. J. Sumakeris, A. K. Agarwal, and J. W. Palmour, "12 kV 4H-SiC p-IGBTs with Record Low Specific On-Resistance," *Materials Science Forum,* vol. 600-603, pp. 1187-1190, Sep. 2008, doi: 10.4028/www.scientific.net/MSF.600-603.1187.

[19] X. Wang and J. A. Cooper, "High-Voltage n-Channel IGBTs on Free-Standing 4H-SiC Epilayers," *IEEE Trans. Electron Devices,* vol. 57, no. 2, pp. 511-515, Jan. 2010, doi: 10.1109/TED.2009.2037379.

[20] S. H. Ryu, L. Cheng, S. Dhar, C. Capell, C. Jonas, J. Clayton, M. Donofrio, M. J. O'Loughlin, A. A. Burk, A. K. Agarwal, and J. W. Palmour, "Development of 15 kV 4H-SiC IGBTs," *Materials Science Forum,* vol. 717-720, pp. 1135-1138, May 2012, doi: 10.4028/www.scientific.net/MSF.717-720.1135.

[21] S. Ryu, C. Capell, C. Jonas, L. Cheng, M. O. Loughlin, A. Burk, A. Agarwal, J. Palmour, and A. Hefner, "Ultra high voltage (>12 kV), high performance 4H-SiC IGBTs," in *Proc. 24th Int. Symp. Power Semiconductor Devices and IC's (ISPSD)*, Jun. 2012, pp. 257-260, doi: 10.1109/ISPSD.2012.6229072.

[22] S. Katakami, H. Fujisawa, K. Takenaka, H. Ishimori, S. Takasu, M. Okamoto, M. Arai, Y. Yonezawa, and K. Fukuda, "Fabrication of a P-Channel SiC-IGBT with High Channel Mobility," *Materials Science Forum,* vol. 740-742, pp. 958-961, Jan. 2013, doi: 10.4028/www.scientific.net/MSF.740-742.958.

[23] S. Ryu, C. Capell, C. Jonas, Y. Lemma, M. O. Loughlin, J. Clayton, E. V. Brunt, K. Lam, J. Richmond, A. Burk, D. Grider, S. Allen, J. Palmour, A. Agarwal, A. Kadavelugu, and S. Bhattacharya, "Ultra high voltage IGBTs in 4H-SiC," in *The 1st IEEE Workshop on Wide Bandgap Power Devices and Applications*, Oct. 2013, pp. 36-39, doi: 10.1109/WiPDA.2013.6695557.

[24] Y. Yonezawa, T. Mizushima, K. Takenaka, H. Fujisawa, T. Kato, S. Harada, Y. Tanaka, M. Okamoto, M. Sometani, D. Okamoto, N. Kumagai, S. Matsunaga, T. Deguchi, M. Arai, T. Hatakeyama, Y. Makifuchi, T. Araoka, N. Oose, T. Tsutsumi, M. Yoshikawa, K. Tatera, M. Harashima, Y. Sano, E. Morisaki, M. Takei, M. Miyajima, H. Kimura, A. Otsuki, K. Fukuda, H. Okumura, and T. Kimoto, "Low Vf and highly reliable 16 kV ultrahigh voltage SiC flip-type n-channel implantation and epitaxial IGBT," in *IEDM Tech. Dig.*, Dec. 2013, pp. 6.6.1-6.6.4, doi: 10.1109/IEDM.2013.6724576.

[25] E. V. Brunt, L. Cheng, M. O. Loughlin, C. Capell, C. Jonas, K. Lam, J. Richmond, V. Pala, S. Ryu, S. T. Allen, A. A. Burk, J. W. Palmour, and C. Scozzie, "22 kV, 1 cm^2, 4H-SiC n-IGBTs with improved conductivity modulation," in *Proc. 26th Int. Symp. Power Semiconductor Devices and IC's (ISPSD)*, Jun. 2014, pp. 358-361, doi: 10.1109/ISPSD.2014.6856050.

[26] T. Deguchi, T. Mizushima, H. Fujisawa, K. Takenaka, Y. Yonezawa, K. Fukuda, H. Okumura, M. Arai, A. Tanaka, S. Ogata, T. Hayashi, K. Nakayama, K. Asano, S. Matsunaga, N. Kumagai, and M. Takei, "Static and dynamic performance evaluation of >13 kV SiC p-channel IGBTs at high temperatures," in *Proc. 26th Int. Symp. Power Semiconductor Devices and IC's (ISPSD)*, Jun. 2014, pp. 261-264, doi: 10.1109/ISPSD.2014.6856026.

[27] Y. Yonezawa, T. Mizushima, K. Takenaka, H. Fujisawa, T. Deguchi, T. Kato, S. Harada, Y. Tanaka, D. Okamoto, M. Sometani, M. Okamoto, M. Yoshikawa, T. Tsutsumi, Y. Sakai, N. Kumagai, S. Matsunaga, M. Takei, M. Arai, T. Hatakeyama, K. Takao, T. Shinohe, T. Izumi, T. Hayashi, K. Nakayama, K. Asano, M. Miyajima, H. Kimura, A. Otsuki, K. Fukuda, H. Okumura, and T. Kimoto, "Device Performance and Switching Characteristics of 16 kV Ultrahigh-Voltage SiC Flip-Type n-Channel IE-IGBTs," *Materials Science Forum,* vol. 821-823, pp. 842-846, June 2015, doi: 10.4028/www.scientific.net/MSF.821-823.842.

[28] E. van Brunt, L. Cheng, M. J. O'Loughlin, J. Richmond, V. Pala, J. W. Palmour, C. W. Tipton, and C. Scozzie, "27 kV, 20 A 4H-SiC n-IGBTs," *Materials Science Forum,* vol. 821-823, pp. 847-850, June 2015, doi: 10.4028/www.scientific.net/MSF.821-823.847.

[29] S. Chowdhury, C. Hitchcock, Z. Stum, R. Dahal, I. B. Bhat, and T. P. Chow, "4H-SiC n-Channel Insulated Gate Bipolar Transistors on (0001) and (000-1) Oriented Free-Standing n− Substrates," *IEEE Electron Device Lett.,* vol. 37, no. 3, pp. 317-320, Jan. 2016, doi: 10.1109/LED.2016.2521164.

[30] N. Watanabe, H. Yoshimoto, A. Shima, R. Yamada, and Y. Shimamoto, "6.5 kV n-Channel 4H-SiC IGBT with Low Switching Loss Achieved by Extremely Thin Drift Layer," *Materials Science Forum,* vol. 858, pp. 939-944, May 2016, doi: 10.4028/www.scientific.net/MSF.858.939.

[31] S. Chowdhury and T. P. Chow, "Performance tradeoffs for ultra-high voltage (15 kV to 25 kV) 4H-SiC n-channel and p-channel IGBTs," in *Proc. 28th Int. Symp. Power Semiconductor Devices and IC's (ISPSD)*, Jun. 2016, pp. 75-78, doi: 10.1109/ISPSD.2016.7520781.

[32] T. Hiyoshi and T. Kimoto, "Reduction of Deep Levels and Improvement of Carrier Lifetime in n-Type 4H-SiC by Thermal Oxidation," *Applied Physics Express,* vol. 2, p. 041101, 2009, doi: 10.1143/apex.2.041101.

[33] T. Okuda, T. Miyazawa, H. Tsuchida, T. Kimoto, and J. Suda, "Enhancement of carrier lifetime in lightly Al-doped p-type 4H-SiC epitaxial layers by combination of thermal oxidation and hydrogen annealing," *Applied Physics Express,* vol. 7, no. 8, p. 085501, 2014, doi: 10.7567/apex.7.085501.

[34] M. Rahimo, A. Kopta, S. Eicher, N. Kaminski, F. Bauer, U. Schlapbach, and S. Linder, "Extending the boundary limits of high voltage IGBTs and diodes to above 8 kV," in *Proc. 14th Int. Symp. Power Semiconductor Devices and IC's (ISPSD)*, Jun. 2002, pp. 41-44, doi: 10.1109/ISPSD.2002.1016166.

[35] F. Niedernostheide, H. Schulze, U. Kellner-Werdehausen, R. Barthelmess, J. Przybilla, R. Keller, H. Schoof, and D. Pikorz, "13-kV rectifiers: studies on diodes and asymmetric thyristors," in *Proc. 15th Int. Symp. Power Semiconductor Devices and IC's (ISPSD)*, Apr. 2003, pp. 122-125, doi: 10.1109/ISPSD.2003.1225245.

[36] H. Schulze, F. Niedernostheide, U. Kellner-Wedehausen, and C. Scheider, "Experimental and numerical investigations of 13-kV diodes and asymmetric light-triggered thyristors," in *European Conference on Power Electronics and Applications*, Sep. 2005, pp. P.1-P.7, doi: 10.1109/EPE.2005.219296.

[37] A. Ito and I. Omura, "13kV UHV-IGBT: Feasibility Study," in *Proc. 32nd Int. Symp. Power Semiconductor Devices and IC's (ISPSD)*, Sep. 2020, pp. 50-53, doi: 10.1109/ISPSD46842.2020.9170034.

[38] A. Nakagawa, "Theoretical Investigation of Silicon Limit Characteristics of IGBT," in *Proc. 18th Int. Symp. Power Semiconductor Devices and IC's (ISPSD)*, Jun. 2006, pp. 1-4, doi: 10.1109/ISPSD.2006.1666057.

[39] M. Naito, H. Matsuzaki, and T. Ogawa, "High current characteristics of asymmetrical p-i-n diodes having low forward voltage drops," *IEEE Trans. Electron Devices,* vol. 23, no. 8, pp. 945-949, Aug. 1976, doi: 10.1109/T-ED.1976.18514.

[40] L. W. Davies, "Electron-Hole Scattering at High Injection-Levels in Germanium," *Nature,* vol. 194, p. 762, May 1962, doi: 10.1038/194762a0.

[41] C. Seok Cheow, "Numerical analysis of a forward-biased step-junction P-L-N diode," *IEEE Trans. Electron Devices,* vol. 18, no. 8, pp. 574-586, Aug. 1971, doi: 10.1109/T-ED.1971.17244.

[42] H. D. Barber, "Effective mass and intrinsic concentration in silicon," *Solid-State Electronics,* vol. 10, no. 11, pp. 1039-1051, Nov. 1967, doi: 10.1016/0038-1101(67)90122-0.

[43] N. D. Arora, J. R. Hauser, and D. J. Roulston, "Electron and hole mobilities in silicon as a function of concentration and temperature," *IEEE Trans. Electron Devices,* vol. 29, no. 2, pp. 292-295, Feb. 1982, doi: 10.1109/T-ED.1982.20698.

[44] M. Roschke and F. Schwierz, "Electron mobility models for 4H, 6H, and 3C SiC," *IEEE Trans. Electron Devices,* vol. 48, no. 7, pp. 1442-1447, Jul. 2001, doi: 10.1109/16.930664.

[45] M. Shur, S. Rumyantsev, and M. Levinshtein, *SiC Materials and Devices : Volume 1* vol. 40, 2006. doi: 10.1142/6134.

[46] T. Kimoto, K. Yamada, H. Niwa, and J. Suda, "Promise and Challenges of High-Voltage SiC Bipolar Power Devices," *Energies,* vol. 9, no. 11, Nov. 2016, doi: 10.3390/en9110908.

[47] J. Lutz, H. Schlangenotto, U. Scheuermann, and R. De Doncker, *Semiconductor power devices: Physics, characteristics, reliability*, 2018. doi: 10.1007/978-3-319-70917-8.

[48] B. J. Baliga, *Fundamentals of power semiconductor devices*: New York, NY, USA, Springer, 2016.

[49] M. Tanaka and A. Nakagawa, "Conductivity modulation in the channel inversion layer of very narrow mesa IGBT," in *Proc. 29th Int. Symp. Power Semiconductor Devices and IC's (ISPSD)*, May 2017, pp. 61-64, doi: 10.23919/ISPSD.2017.7988893.

[50] P. Luo, H. Y. Long, and E. M. S. Narayanan, "A Novel Approach to Suppress the Collector-Induced Barrier Lowering Effect in Narrow Mesa IGBTs," *IEEE Electron Device Letters,* vol. 39, no. 9, pp. 1350-1353, Sep. 2018, doi: 10.1109/LED.2018.2854363.

[51] H. Feng, W. Yang, Y. Onozawa, T. Yoshimura, A. Tamenori, and J. K. O. Sin, "A 1200 V-class Fin P-body IGBT with ultra-narrow-mesas for low conduction loss," in *Proc. 28th Int. Symp. Power Semiconductor Devices and IC's (ISPSD)*, Jun. 2016, pp. 203-206, doi: 10.1109/ISPSD.2016.7520813.

[52] I. Deviny, H. Luo, Q. Xiao, Y. Yao, C. Zhu, L. Ngwendson, H. Xiao, X. Dai, and G. Liu, "A novel 1700V RET-IGBT (recessed emitter trench IGBT) shows record low VCE(ON), enhanced current handling capability and short circuit robustness," in *2017 29th International Symposium on Power Semiconductor Devices and IC's (ISPSD)*, May 2017, pp. 147-150, doi: 10.23919/ISPSD.2017.7988932.

[53] L. Ngwendson, I. Deviny, C. Zhu, I. Saddiqui, C. Kong, A. Islam, J. Hutchings, J. Thompson, M. Briggs, O. Basset, H. Luo, Y. Wang, and Y. Yao, "Extending the RET-IGBT (recessed emitter trench IGBT) concept to high voltages: Experimental demonstration of 3.3kV RET IGBT," in *2018 IEEE 30th International Symposium on Power Semiconductor Devices and ICs (ISPSD)*, May 2018, pp. 140-143, doi: 10.1109/ISPSD.2018.8393622.

[54] L. Ngwendson, I. Deviny, C. Zhu, I. Saddiqui, J. Hutchings, C. Kong, Y. Wang, and H. Luo, "New Locos Trench Oxide IGBT Enables 25% Higher Current Density in 4.5kV/1500A Module," in *Proc. 31th Int. Symp. Power Semiconductor Devices and IC's (ISPSD)*, May 2019, pp. 323-326, doi: 10.1109/ISPSD.2019.8757651.

[55] C. Papadopoulos, B. Boksteen, M. Andenna, D. Prindle, E. Buitrago, S. Hartmann, S. Matthias, C. Corvasce, F. Bauer, M. Bellini, U. Vemulapati, G. Paques, R. Schnell, A. Kopta, and M. Rahimo, "The Third Generation 6.5 kV HiPak2 Module Rated 1000 A and 150 °C," in *PCIM Europe 2018; International Exhibition and Conference for Power Electronics, Intelligent Motion, Renewable Energy and Energy Management*, Jun. 2018, pp. 1-8.

[56] L. Cheng, A. Agarwal, M. O. Loughlin, C. Capell, A. Burk, J. Palmour, A. Ogunniyi, H. O. Brien, and C. Scozzie, "Advanced silicon carbide gate turn-off thyristor for energy conversion and power grid applications," in *IEEE Energy Conversion Congress and Exposition (ECCE)*, Sep. 2012, pp. 2249-2252, doi: 10.1109/ECCE.2012.6342435.

[57] L. Cheng, A. K. Agarwal, C. Capell, M. O. Loughlin, K. Lam, J. Richmond, E. V. Brunt, A. Burk, J. W. Palmour, H. O. Brien, A. Ogunniyi, and C. Scozzie, "20 kV, 2 cm^2, 4H-SiC gate turn-off thyristors for advanced pulsed power applications," in *19th IEEE Pulsed Power Conference (PPC)*, Jun. 2013, pp. 1-4, doi: 10.1109/PPC.2013.6627403.

[58] M. A. Rezaei, G. Wang, A. Q. Huang, L. Cheng, and C. Scozzie, "Static and dynamic characterization of a >13kV SiC p-ETO device," in *Proc. 26th Int. Symp. Power Semiconductor Devices and IC's (ISPSD)*, Jun. 2014, pp. 354-357, doi: 10.1109/ISPSD.2014.6856049.

[59] X. Song, A. Q. Huang, M. Lee, C. Peng, L. Cheng, H. O. Brien, A. Ogunniyi, C. Scozzie, and J. Palmour, "22 kV SiC Emitter turn-off (ETO) thyristor and its dynamic performance including SOA," in *Proc. 27th Int. Symp. Power Semiconductor Devices and IC's (ISPSD)*, May 2015, pp. 277-280, doi: 10.1109/ISPSD.2015.7123443.

[60] T. Kato, Y. Fukuoka, H. Kang, K. Hamada, A. Onogi, H. Fujiwara, T. Ito, T. Kimoto, and F. Udrea, "Enhanced Performance of 50 nm Ultra-Narrow-Body Silicon Carbide MOSFETs based on FinFET effect," in *Proc. 32nd Int. Symp. Power Semiconductor Devices and IC's (ISPSD)*, Sep. 2020, pp. 62-65, doi: 10.1109/ISPSD46842.2020.9170182.

[61] *Silvaco Atlas User's Manual* Santa Clara, CA: Silvaco, Inc., 2016.

[62] M. Kitagawa, I. Omura, S. Hasegawa, T. Inoue, and A. Nakagawa, "A 4500 V injection enhanced insulated gate bipolar transistor (IEGT) operating in a mode similar to a thyristor," in *IEDM Tech. Dig.*, Dec. 1993, pp. 679-682, doi: 10.1109/IEDM.1993.347221.